Harnessing harmonics for imaging thin shallow reflectors

Christopher B. Harrison, Gary Margrave, Michael Lamoureux, Arthur Siewert, Andrew Barrett and Helen Isaac

ABSTRACT

Harmonics have traditionally been treated as noise to be attenuated out of the vibrator seismic data. Much time and energy have been dedicated to the removal of these harmonics in all stages of seismic delving, from the acquisition phase, to data processing and even vibrator engineering. This desire to remove the frequencies associated with higher order harmonics comes from the correlation process which causes ghost forerunners or tails at positive and negative correlation times (depending on type of sweep) if harmonically "contaminated" sweeps are used as correlation operators. However, these higher frequencies, if sampled properly and harmonics extracted precisely, prove to be highly useful as correlation operators to image thin near surface reflectors. In this paper we utilize harmonics decomposed from baseplate recorded sweeps and ground force as correlation operators. The results indicate that the baseplate harmonics reveal thinner near surface reflectors while the ground force reveals more numerous coherent near surface reflections.

Introduction

In 2010 Statoil acquired a high resolution vibroseis seismic line with the intention of harnessing the harmonics generated by the vibrator for near surface imaging. The parameters of the survey were designed to finely sample the wavefield, ensuring that the frequency content from higher order harmonics could be reclaimed as signal instead of being attenuated as noise. The survey was acquired uncorrelated with the forethought that the harmonic frequency content within the sweeps could be decomposed and used as correlation operators. Parameters for the high resolution survey are outlined in Harrison et al. (2012) and reproduced in Table 1.

Table 1. Survey and sweep parameters.

Sweep Parameters	
Length	20 s
Function	Non-linear, High Dwell
Frequency	6 – 240 Hz
Taper – cosine	300ms (start) – 300ms (end)
Sampling	0.5 ms
Boost	0.09 dB/Hz
Source Type	
Model	Envirovibe
Unit Weight	12500 lbs
Number of Vibes	1
Survey Parameters	
SX	3m
RX	12m
Max # Traces	192
Receiver type	Marsh

In 2011 CREWES, POTSI and Statoil began work on designing algorithms to decompose harmonics from a harmonically "contaminated" sweep. Least squares methodology and the Gabor transform were employed to decompose higher order harmonics from both synthetic and field sweeps. Two general methods were devised and coined: time dependant Gabor decomposition (TDGD) and frequency dependent Gabor decomposition (FDGD). A complete understanding of the theory for TDGD and FDGD can be found in Harrison et al. (2011). Both these methods are able to decompose the first harmonic, or fundamental (H1), to the ninth harmonics (H9) from a sweep containing harmonics. H9 is currently the decomposition limit of our algorithms.

In 2012, however, we were not completely sure which of the two methods provided the most accurate harmonic results. Error calculations pointed towards TDGD as having an advantage, albeit slight, over FDGD. The preliminary processing by Harrison et al. (2012) using both synthetic and field data also indicated that TDGD had an advantage over FDGD. However, this aforementioned conclusion was based on the results of only two seismic images. What we eventually find is that FDGD has a minor frequency advantage over its TDGD sibling.

The harnessing of harmonics

Harrison et al. (2012) discussed the theoretical and practical methods for using harmonics as correlation operators. In that study we used TDGD and FDGD to extract a total of 67572 harmonics (H1 to H9) from two separate sweep records over 1877 sweep points. The records were the sweeps recorded at the baseplate (BP) and the weight-sum, or ground force (GF). We recombined the decomposed harmonics at each sweep point to create a composite sweep adding an addition 3754 sweeps to the fray. In the 2012 CREWES paper we only had time to create a pilot correlated image and a single image resulting from using H2 TDGD as extracted from a BP recorded sweep. The processing flow used by Harrison et al. (2012) with a slight modification at the end is reproduced in Table 2.

Table 2. Basic processing flow for correlation using the pilot sweep.

Processing	Pilot	Other
Correlation	✓	✓
Geometry	✓	Pilot
Gabor Deconvolution.	✓	✓
Velocity Analysis 1	✓	
Velocity Analysis 2	✓	Pilot
Apply Residual Statics	✓	Pilot
NMO	✓	✓
CDP Stack	✓	✓
Kirchhoff Time Mig. (100 Hz)	✓	Pilot
f-x Deconvolution (300 Hz)	✓	✓

The modification to the processing flow is the f-x deconvolution at the end of the flow which was added to balance signal and noise. A word of caution to CREWES sponsors who have access to the CREWES Promax module library and want to produce similar results to the research presented here. Using the CREWES Promax module "Gabor" took roughly 96-106 hours to run. Please note that "Gabor2" should be used instead. This later module took approximately 3 hours to run with results being near identical to the original "Gabor" module. The lesson learned is to speak directly to the developer of an algorithm (Dave Henley in this case) to see if he or she has an updated version of a module. All but five images listed in Table 3 were produced using Gabor2 for an approximate total of 3400 hours (141 days... not all concurrent) for processing time.

The columns of Table 2 represent the two ways the data presented in this paper were processed. The first column or "Pilot" shows the initial processing which utilized the pilot sweep as the correlation operator. The image produced using this flow is shown in Figure 1. This image is used as the primer by which to judge the subsequent images generated using harmonics as correlation operators. Annotations on the right side of Figure 1 show the locations of key horizons in the area.

In the bottom left hand side of Figure 1 is a plot which contains the amplitude spectrum of the pilot image (black) with respect to the white bounding box between 50 and 300 ms. The faint red line in the plot represents the pilot image prior to any filtering. This amplitude plot appears on all full images reproduced in this paper. These horizons are interpreted and confirmed by Statoil.

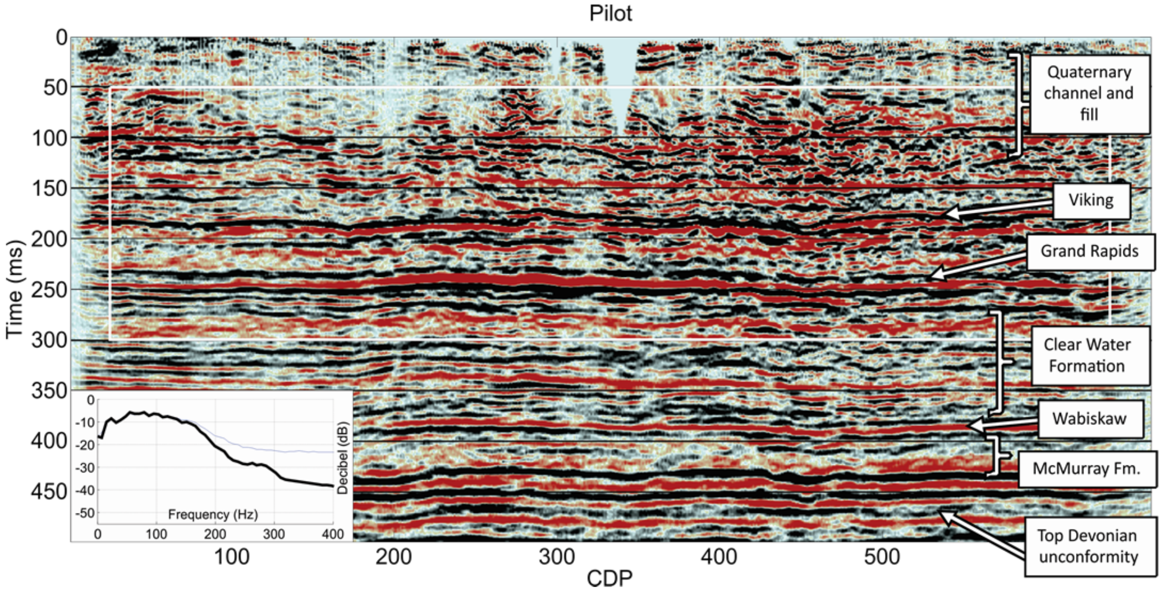

Figure 1. The pilot correlated image with annotations.

Column two of Table 2 ("Other") refers to how all harmonically correlated seismic images were produced. The only difference between the pilot flow and the "other" flow is the correlation operator used at step one. Table 3 lists the bulk of the harmonically correlated images produced using the processing flow in Table 2. In the case of the Pilot, Synth H2, and Synth H3, their respective correlation operators were the same for all 1877 sweep points. The remaining images in Table 3 used different correlation operators at each 1877 sweep point. The H_n+H_{n+1} are additions of mean scaled harmonics prior to correlation. Comp., or composite, is a sweep where all harmonics (H1 to H9) were added together prior to correlation. No scaling was applied to these harmonics.

Table 3. Checkist of all seismic images generated.

Type	H1	H2	H3	H1+H2	H2+H3	H1+H2+H3	Comp.
Pilot	Pilot	Synth.	Synth.	✓	✓	✓	-
Base Plate							
TDGD	✓	✓	✓	✓	✓	✓	✓
FDGD	✓	✓	✓	✓	✓	✓	✓
Ground Force							
TDGD	✓	✓	✓	✓	✓	✓	✓
FDGD	✓	✓	✓	✓	✓	✓	✓

Of course not all images checked off in Table 3 are reproduced in this paper. Six full images are reproduced below with two more figures showing image slices for comparison purposes.

Imaging Results

The pilot correlated image shown in Figure 1 will be considered the primer by which all harmonically correlated images will be judged. The time-depth has been truncated to 500 ms in order to focus on the near surface where harmonics have not been attenuated due to spreading or absorption of their higher frequencies. Table 4 lists the harmonically correlated image reproduced in this paper. FDGD was chosen over TDGD for comparison purposes both for brevity in figure reproduction and a slight frequency content advantage tipping the scales for FDGD. Future research should include TDGD results for analysis.

Table 4. List of full images reproduced in this paper.

Type	H1	H2	H3
Base Plate			
FDGD	Figure 2	Figure 3	Figure 4
Ground Force			
FDGD	Figure 5	Figure 6	Figure 7

The six images in Table 4 have been reproduced in full to illustrate the effect each different harmonic has had on imaging when compared to pilot primer (Figure 1). The BP images appear to have revealed the thinnest reflections with respect to the Grand Rapids (250 ms), Viking (200 ms) and Quaternary channel (0 – 150 ms). The BP images render two or even three dipoles on these horizons where the GF and pilot images appear to render only one dipole. This increase in thin reflector resolution is due to the striking frequency content difference between the BP and GF images.

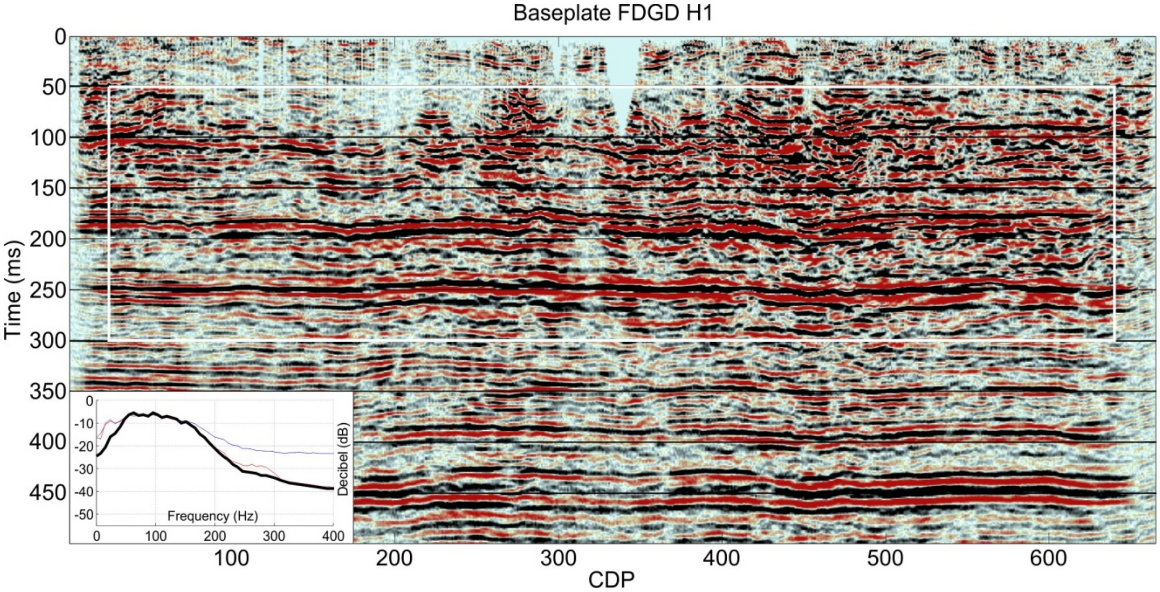

Figure 2. Baseplate FDGD H1 imaging results

The amplitude spectrum of BP H2 (Figure 3) and BP H3 (Figure 4) is more pronounced in the higher frequencies (100 - 300 Hz) while GF H2 (Figure 6) and GF H3 (Figure 7) are more pronounced on the lower frequencies (under 100 Hz). This substantial increase in higher frequencies of the BP harmonically correlated images has translated into resolving thinner shallower reflections.

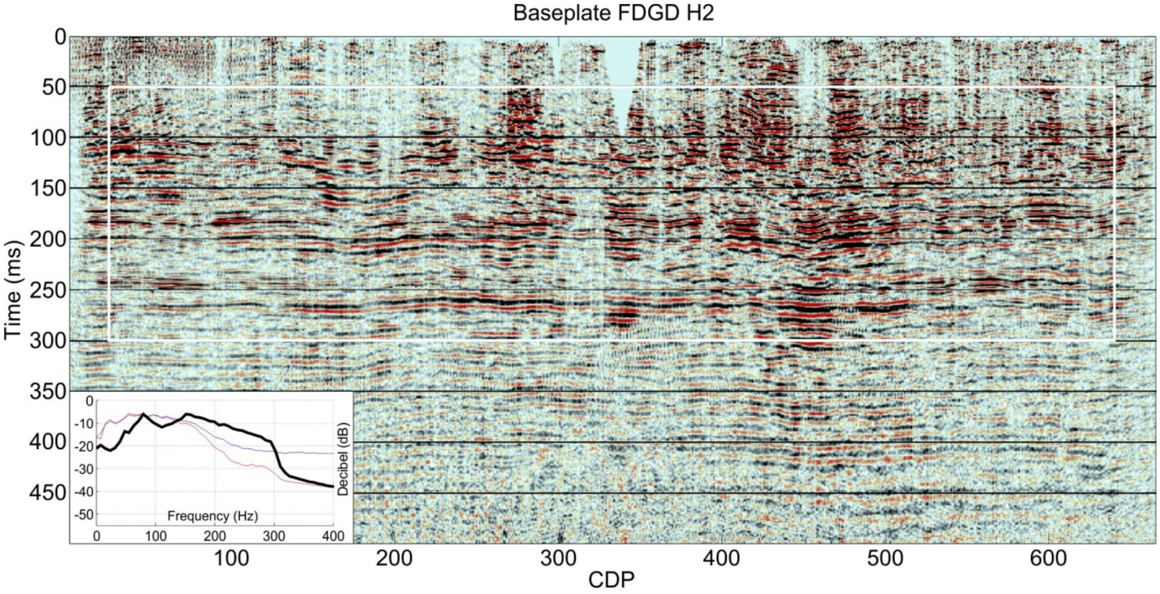

Figure 3. Baseplate FDGD H2 imaging results

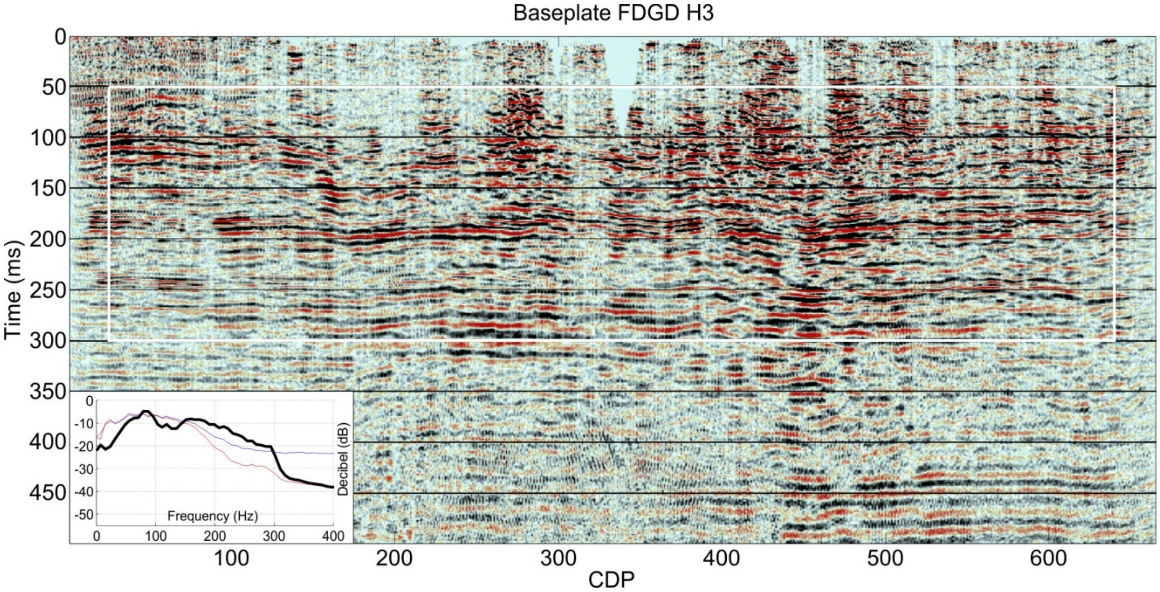

Figure 4. Baseplate FDGD H3 imaging results

This frequency difference between the BP and GF correlated images does not automatically relegate the GF to being less useful however. The GF correlated images do produce more numerous coherent reflectors than their BP siblings. This difference in frequency content and imaging results could explain different aspects of the stratigraphy in the region. Future research should still take into consideration both the BP and GF harmonically correlated images for a full analysis of the subsurface.

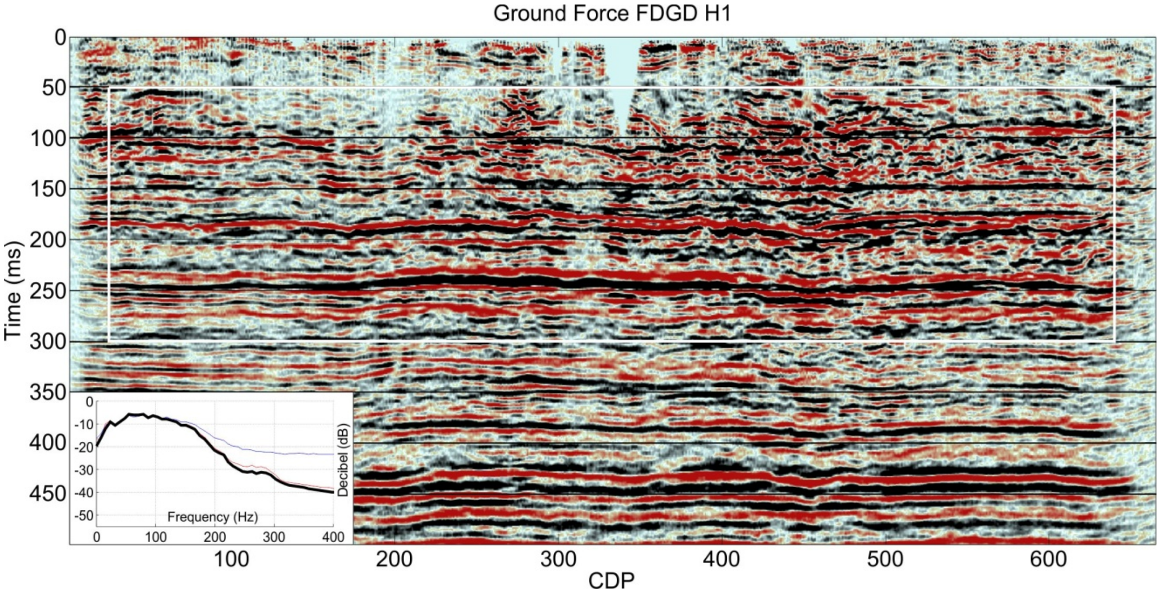

Figure 5. Ground force FDGD H1 imaging results

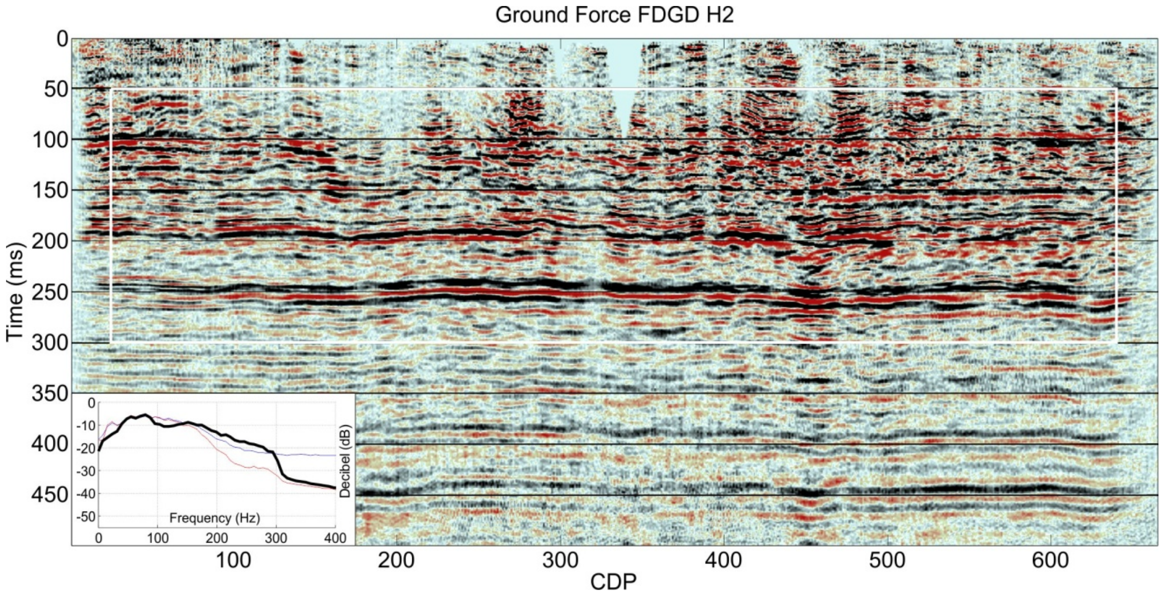

Figure 6. Ground force FDGD H2 imaging results.

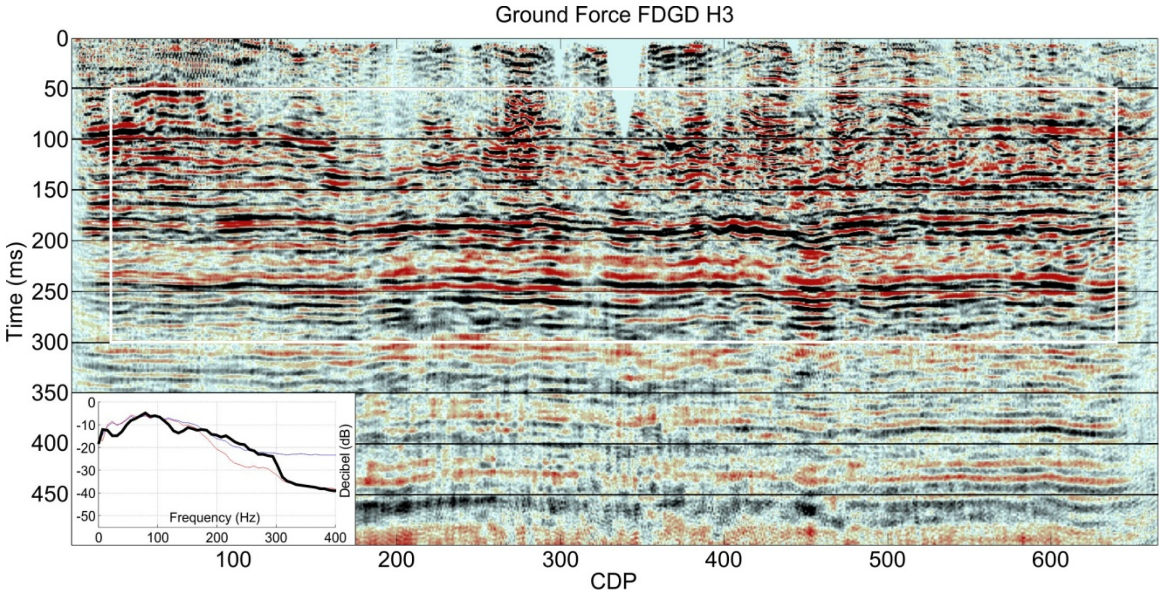

Figure 7. Ground force FDGD H3 imaging results.

Two final images have been created to juxtapose imaging results for both BP and GF. Figure 8 shows the BP harmonically correlated images slices using H1, H2, H3 and a H2+H3 compared to the pilot image (far left). Figure 9 shows the GF harmonically correlated images slices using H1, H2, H3, and H2+H3. Both these images (Figure 8 and Figure 9) provide good evidence that using harmonics extracted from the BP recorded sweep using FDGD have indeed imaged thin shallow reflectors.

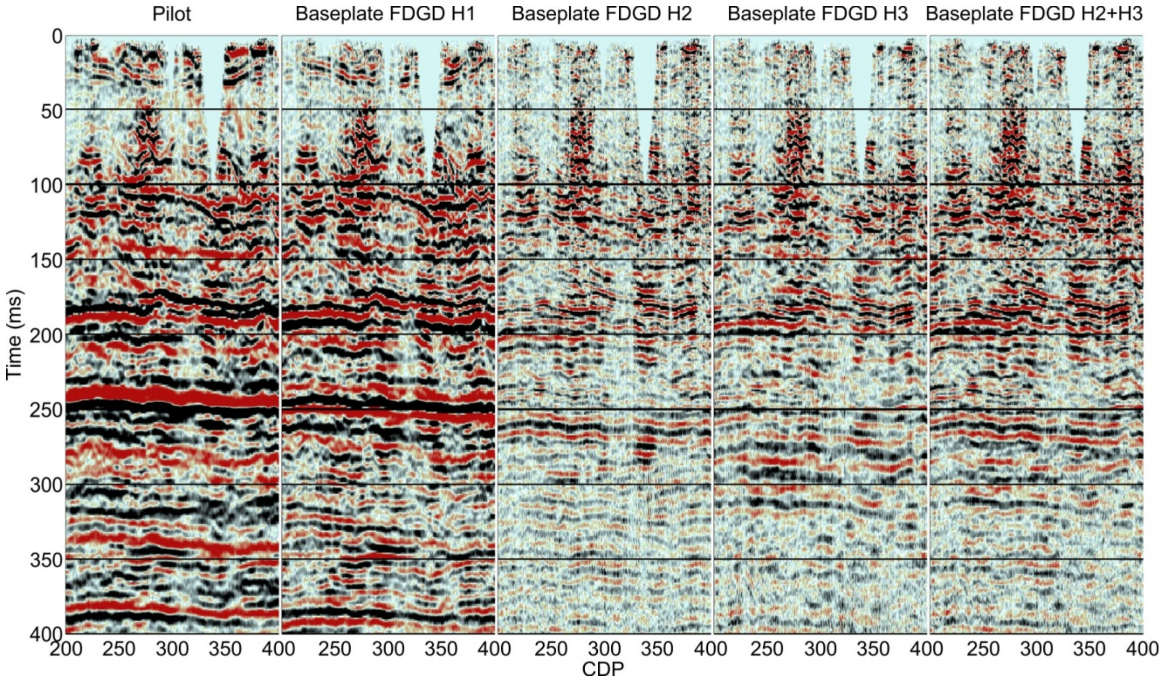

Figure 8. The pilot image slice compared to the baseplate FDGD H1, H2, H3 and H2+H3.

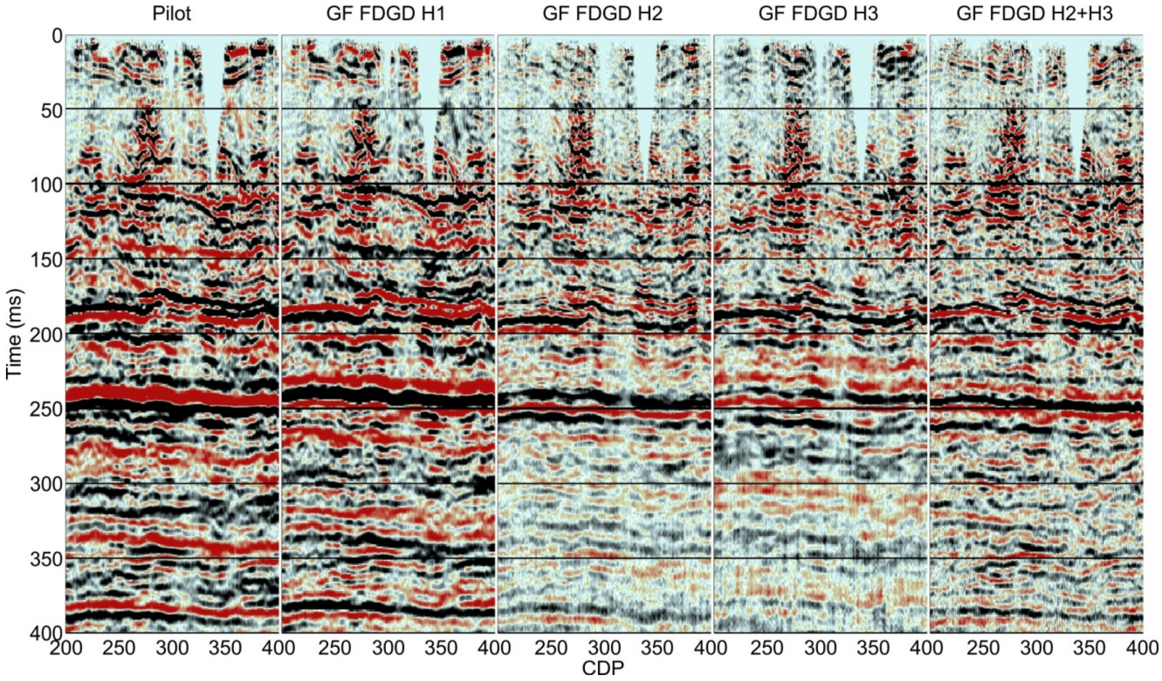

Figure 9. The pilot image slice compared to the ground force FDGD H1, H2, H3 and H2+H3.

Conclusions

Harmonics as generated during vibrator seismic acquisition have traditionally been treated as noise to be attenuated from the acquisition phase, data processing and vibrator engineering. However, the higher frequency associated with these harmonics no longer need be considered undesirable. We have shown the results of using harmonics extracted from the baseplate recorded sweep and ground force as correlation operators for seismic imaging. These imaging results indicated that H2, H3 and H2+H3 as extracted from the BP recorded sweep using FDGD revealed a sizeable number of thinner near surface reflectors.

Future Work

- Phase lag between pilot primer and all harmonically correlated images
- H4 and H5 as correlation operators!(?)

Acknowledgements

We would like to thank CMC (Carbon Management Canada) for making the last few months of this project possible. We also would like to thank Mprime, NSERC, CREWES, POTSI and their sponsors for their continued commitment to supporting outstanding geophysical research. We would also like to thank StatOil for their support.

References

Harrison, C. B., Margrave, G. F., Lamoureux, M. P., Siewert, A., and Barrett, A. (2011). "Harmonic decomposition of vibroseis sweeps using Gabor analysis." CREWES Research Report **2011**.

Harrison, C. B., Margrave, G. F., Lamoureux, M.P., Siewert, A., Barrett, A. and Isaac, J.H. (2012). "Towards using harmonic "contamination" as signal for thin reflectors." CREWES Research Report **2012**.